JOURNAL OF Materials CHEMISTRY

Structure of composites $A_{1+x}(A'_xB_{1-x})O_3$ related to the 2H hexagonal perovskite: relation between composition and modulation

J. M. Perez-Mato,[a] M. Zakhour-Nakhl,[b] F. Weill*[b] and J. Darriet[b]

[a]*Departamento de Física de la Materia Condensada, Facultad de Ciencias, Universidad del Pais Vasco, Apdo 644, 48080 Bilbao, Spain*
[b]*Institut de Chimie de la Matière Condensée de Bordeaux (ICMCB), Avenue du Dr. Schweitzer, 33608 Pessac Cedex, France*

Received 10th May 1999, Accepted 8th September 1999

An idealized structural model is proposed for materials closely related to the 2H hexagonal perovskite and with general formula $A_{3n+3m}A'_nB_{3m+n}O_{9m+6n}$ {or $A_{1+x}(A'_xB_{1-x})O_3$, $x=[0, 1/2]$}. The structures of all these compounds, considered as commensurate or incommensurate modulated composites, can be described in a first approximation by a unique structure in the superspace formalism with occupational Crenel functions and sawtooth displacive modulations along the trigonal axis. The structural modulation has only two variable parameters: the modulation wave vector or misfit parameter, which is fixed by the compound composition, and the height difference between the octahedra and triangular prisms of O_6 present in the trigonal $[A',B]O_3$ columns of the structure. Just by varying these parameters, the basic structural features of any compound with arbitrary composition parameter x are reproduced, including the two limiting cases ABO_3 (2H perovskite) and $A_3A'BO_6$. For instance, the sequence of octahedra and prisms along the $[A',B]O_3$ columns can be considered a generalized Fibonacci chain and its dependence on composition follows a Farey tree rule which comes out directly from the model. A comparison with available experimental data, and in particular with some fully determined structures, demonstrates the soundness of the proposed scheme as a reference for such structures and the best starting point for their refinement. The model, although developed within the superspace formalism, is closely related to the polytype layer picture in direct space. The present structural analysis constitutes a new example of the efficiency of the 4-dimensional superspace formalism for describing in a unified form the structures of so-called 'composition flexible' systems.

1 Introduction

It is well known that the structure of the hexagonal perovskite ABO_3 can be described by the stacking along the c-direction of compact layers of composition $[AO_3]$. This stacking creates octahedral $[O_6]$ sites which share faces and are occupied by the B cations. In recent work, Darriet and Subramanian[1] have been interested in related structures resulting from the stacking along the c-direction of mixed layers $[A_3O_9]$ and $[A_3A'O_6]$. The latter derives from the $[A_3O_9]$ layer by substituting one A′ atom for three oxygen atoms (Fig. 1). The stacking of these mixed layers creates prismatic sites with triangular bases and leads to a new family of phases with a general formula which can be written as $A_{3n+3m}A'_nB_{3m+n}O_{9m+6n}$ where n/m is the ratio between the number of layers of $[A_3A'O_6]$ and $[A_3O_9]$. The structures of all the phases belonging to this family are characterised by a parameter a of around 10 Å $\left(a_{\text{perovs}}\sqrt{3}\right)$ and a parameter c which depends on the integers n and m. The main feature of all these structures is the presence of chains of octahedra and trigonal prisms along the c-direction. The B cations are located in the center of the octahedra while the A′ cations lie in the trigonal prisms. The lattice periodicity along z, c_s, depends on the particular stacking of layers realized in each case and, in general, is much larger than the perovskite lattice parameter c_{perovs}. An approximate relation of this parameter c_s with the average thickness of a layer, e, can be deduced from two rather general considerations: in order to obtain an $[A_3A'O_6]$ layer from an $[A_3O_9]$ layer there are three different possibilities of substitution. Hence there are three different types of $[A_3A'O_6]$ layers and as a consequence the total number of $[A_3A'O_6]$ layers in the unit cell must be a multiple of three. As the stacking of the layers is of the hexagonal type, the total number of layers in the unit cell must be even. Consequently four cases can be distinguished:

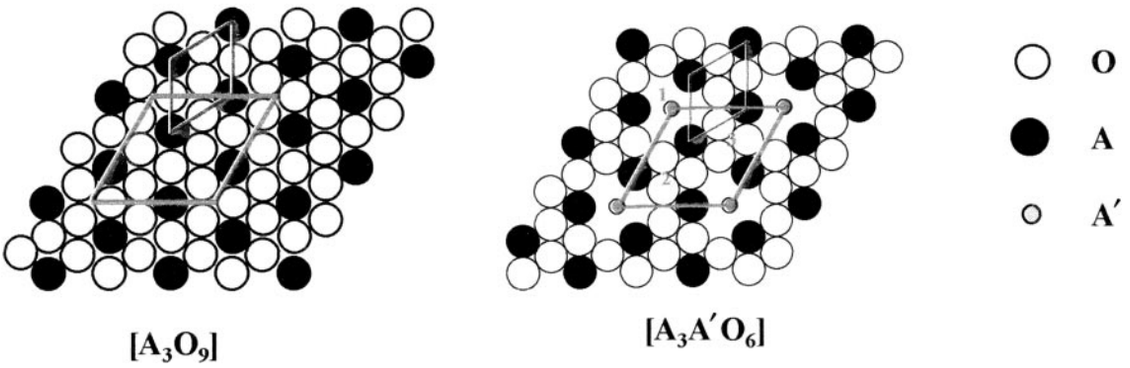

Fig. 1 Schematic view of the $[A_3O_9]$ and $[A_3A'O_6]$ layers.

1. When $n+m$ is even and n is a multiple of 3, then $c_s=(n+m)e$.
2. When $n+m$ is even and n is not a multiple of 3, then $c_s=3(n+m)e$.
3. When $n+m$ is odd and n is a multiple of 3, then $c_s=2(n+m)e$.
4. When $n+m$ is odd and n is not a multiple of 3, then $c_s=6(n+m)e$.

As members of the family, the following list of compounds reported, to date in the literature, can be mentioned:

***m*=1 and *n*=0, $A_3B_3O_9$.** This is the trivial stoichiometry ABO_3, corresponding to the 2H polytype of the hexagonal perovskites. Due to the absence of any $[A_3A'O_6]$ layer the chains are only made of octahedra sharing faces.

***m*=1 and *n*=1, $A_6A'B_4O_{15}$.** Members which have been characterised are $Ba_6Ni_5O_{15}$,[2] $Sr_6Co_5O_{15}$,[3] $Ba_6CuIr_4O_{15}$,[4] $Ba_6ZnIr_4O_{15}$,[4] $Sr_6Rh_5O_{15}$[5] and $Ba_6Mn_4PdO_{15}$.[6] The chains along the *c*-direction are made of tetramers of face-sharing octahedra isolated by a trigonal prism. These phases crystallise in the *R*32 space group. Two different situations can be distinguished: either A′=B (A′=Ni, Co, Rh) or A′≠B. In the former case the B cation formally presents two different oxidation states and lies in both the prismatic and the octahedral sites.

***m*=1 and *n*=2, $A_9A'_2B_5O_{21}$.** The first phase corresponding to this case has been prepared.[7] Originally the stoichiometry of the compound was supposed to be $Sr_9Ni_{6.64}O_{21}$, but recently Evain *et al.*[8] have shown this phase to be $Sr_9Ni_7O_{21}$. The chains are formed of dimers and trimers of octahedra isolated by trigonal prisms.

***m*=1 and *n*=3, $A_4A'B_2O_9$.** The succession of one $[A_3O_9]$ layer and three $[A_3A'O_6]$ layers leads to the formation of dimers of octahedra separated by trigonal prisms. Many examples of this member are already known: $Sr_4Ru_2O_9$,[9] in which the prismatic site is empty (see Fig. 2), $Sr_4CuIr_2O_9$,[10] $Sr_4Ni_3O_9$,[11,12] the solid solution $Ba_{12}(Ba_xPt_{3-x})Pt_6O_{27}$[13] and the phase $Ba_{1.317}(Cu,Pt)O_3$.[14,15]

***m*=0 and *n*=1, $A_3A'BO_6$.** Numerous ternary or quaternary oxides have this structure. The chains are now formed by a sequence of one octahedron and one prism. Examples of such structures include Sr_4PtO_6,[16] Ca_3LiRuO_6,[17] Sr_3LiRuO_6,[17] Ba_4PtO_6,[18] Sr_3MgMO_6 (M=Pt, Ir, Rh)[19] and $NaCa_3MO_6$ (M=Ir, Ru).[20]

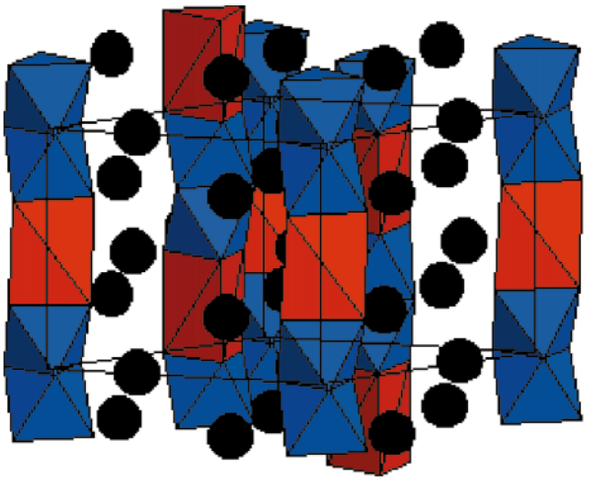

Fig. 2 Average structure of $Sr_4\square Ru_2O_9$ (*n*=3, *m*=1, A′=□). The sequence along the columns is 2 octahedra and 1 prism.

Some more complex cases with *m*>1 can also be cited: $Ba_{16}Cu_3Ir_{10}O_{39}$ (*n*=9, *m*=7),[21] $Ba_{14}Cu_3Ir_8O_{33}$ (*n*=9, *m*=5)[21] and $Ba_5CuIr_3O_{12}$ (*n*=3, *m*=2),[21] $Sr_{14}Co_{11}O_{33}$ (*n* = 9, *m* = 5)[22] and $Sr_{24}Co_{19}O_{57}$ (*n*=5, *m*=3)[22] and $Ba_5Mn_3PdO_{12}$ (*n*=3, *m*=2)[6] and $Ba_7Mn_5PdO_{18}$ (*n*=3, *m*=4).[6]

The general formula of the whole family can be expressed in an equivalent way as $A_{1+x}(A'_xB_{1-x})O_3$ with $x=n/(3m+2n)$, so that when compared with the reference 2H hexagonal perovskite the substitution of B cations by A′+B pairs is emphasized. In this formulation, the composition variable x can be envisaged to be any number between 0 and 1/2.

According to the experimental studies published up to now, some general structural features can be summarized:

(i) The compounds keep the main features of the hexagonal 2H perovskite with the $[A',B]O_3$ groups forming a hexagonal lattice of columns along the *c*-direction and the A cations constitute chains between the $[A',B]O_3$ columns.

(ii) In accordance with the layer model, instead of only octahedra sharing faces, as in the 2H perovskite, the $[A',B]O_3$ systems form columns with a certain sequence of octahedra and trigonal prismatic units (see Fig. 2). As stressed above, the tetravalent B atoms are located within the octahedral O_6 units, while the divalent A′ cations are situated either within the trigonal prisms or are split on their rectangular faces.[11] Thus, the ratio of prisms and octahedra in the chains, $N_{prisms}/N_{octahedra}$, is determined by the ratio of A′ atoms to B atoms in the material, that is $N_{prisms}/N_{octahedra}=x/(1-x)$.

(iii) No general unique rule for the sequence of octahedra and trigonal prisms within the columns has yet been established, although in some cases the layer model favors some particular sequences.[21] Prisms are never consecutive along *z* in a column and neighboring columns have the same sequence but are shifted so that the distribution of prisms along *z* on the three columns surrounding a set of interstitial A cations is rather uniform.

(iv) The geometry of the octahedral and prismatic units along the chains is rather rigid. The sizes of all octahedra (prisms) are similar although this is not, in general, forced by symmetry. The distortions correspond to small rotations of the O_3 triangles on the plane *xy*, while the heights along *z* of the octahedra and prisms may fluctuate slightly from their average values, D_o and D_p, respectively. However, the average height D_p of the prisms is significantly smaller than the value $2D_o$ expected from the ideal layer model.

(v) For compounds with simple compositions, and hence short periods, along *z*, the A atoms in the chains along *z* are normally located either at the level of the center of a triangular prism if it exists on any of the three neighboring $[A',B]O_3$ columns, or at the level of the O_3 triangles in neighboring columns, as expected from the layer model.

When the general formula $A_{1+x}(A'_xB_{1-x})O_3$ is compared with that written in terms of the numbers of layers *n* and *m*, it can be seen that similar compositions (*i.e.* similar values of *x*) correspond in general to quite different values of *n*/*m* and as a consequence to very different cell sizes c_s (and space group symmetries) in the conventional crystallographic description. However, the main features of the diffraction diagram are quite similar for compounds with similar values of the composition 'misfit' *x* (see Fig. 3), and in general the diffraction diagram can be considered to vary continuously with this parameter. A more unifying picture, consistent with these common features, can be obtained if the compounds are described as modulated composites, either commensurate or incommensurate.[23–25] The structure is then depicted as two mutually interacting subsystems,[8,14] modulated along *z* but periodic on the plane *xy*. Subsystem 1 is formed by the $[A',B]O_3$ columns and has an

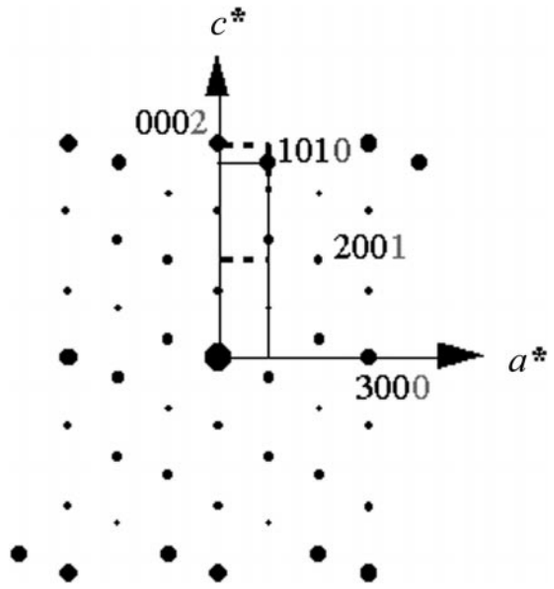

Fig. 3 Schematic diffraction pattern of the composite crystal $A_{1+x}(A'_xB_{1-x})O_3$ on the xz plane, showing the two different reciprocal lattice periodicities along the z-axis and the four integer indexation of the Bragg peaks.

average c-lattice parameter c_1 close to $c_{perovs}/2$, while the average structure of subsystem 2, formed by the A cations, has a c-lattice parameter $c_2 = c_{perovs}$. Thus, the average unit cell of the A subsystem contains twice as many 'molecular' units as the average cell of the $[A',B]O_3$ substructure.[8,14] Therefore, the composition of a given compound can be directly related to the ratio of the c-parameters of the two (average) substructures. For instance a 1:1 composition ratio between the two subsystems would require that $(c_2/2)/c_1 = 1$, while, in general, the composition $1:1+x$ implies that $(c_2/2)/c_1 = 1/(1+x)$. Hence, a mere determination from the experimental diffraction diagram of the ratio $\gamma = c_2^*/c_1^* = c_1/c_2$ between the reciprocal parameters c_1^* and c_2^* is sufficient for deriving the compound composition through the relation[8] $\gamma = (1+x)/2$. According to the range of values of x, the parameter γ in the diffraction diagram can vary between 1/2 and 3/4.

As usual in composite systems, both substructures are modulated along z with a modulation period given by the average c-parameter of the other subsystem, *i.e.* the modulation wave vector of subsystem 1 is c_2^*, and *vice versa*. For many purposes, the two subsystems can be analysed separately in direct space as two independent modulated structures. In Fourier space, however, their diffraction diagrams superpose coherently. An indexation with four indices is normally used (see Fig. 3), so that each Bragg reflection $\boldsymbol{H}$ can be expressed as $\boldsymbol{H} = h\boldsymbol{a}^* + k\boldsymbol{b}^* + l\boldsymbol{c}_1^* + m\boldsymbol{c}_2^* = (h,k,l,m)$ and in general both subsystems contribute to each reflection. Only if the modulations of both subsystems were neglected, the so called 'main' reflections $(h,k,l,0)$ with $l \neq 0$ and $(h,k,0,m)$ with $m \neq 0$ could be interpreted as being Bragg reflections produced exclusively by the subsystems 1 and 2, respectively, while the so called 'authentic satellite' reflections (h,k,l,m) with both l and $m \neq 0$ would not exist. The modulations of both subsystems, however, cause in general the presence of these latter satellites plus non-negligible contributions of both subsystems in both sets of main reflections.

According to the composite description, the structure of a compound $A_{1+x}[A',B]O_3$ would be formally incommensurate only if x has an irrational value (this would correspond to an aperiodic sequence of layers). Indeed, a rational value of x is a necessary and sufficient condition for γ being rational, *i.e.* $\gamma = p/k$, with p and k being integers, and in this case, the composite is formally commensurate with a superstructure unit cell parameter $c_s = c_1 k = c_2 p$. Obviously any experimental value of γ can be identified within experimental resolution with some fraction p/k. In practice, however, an incommensurate approximation can be valid for any fraction p/k with large k.[26] In any case, within the composite approach and its description using the superspace formalism,[24,25,27] the distinction of incommensurate cases with respect to commensurate ones is not essential for a precise structural analysis. In this formalism, the structure factor formula for the commensurate case is always valid and can be used in any case. The incommensurate version of the structure factor expression is a simplification of the general formula for irrational values of γ, which in broad terms is also approximately valid for fractions with large denominators.[26]

The $A_{1+x}[A',B]O_3$ materials can be considered an example of the type of structures pointed out by Withers *et al.* as 'composition flexible structures'.[28] The use of a composite description within the superspace formalism,[24,25,27] relegates the actual ratio γ between the c-parameters of the two substructures and therefore, the particular composition of the system to a secondary role in the description of the structure. Usually, as discussed in ref. 28 with several examples, the symmetry properties (superspace group) and most of the structural parameters in the superspace description of these materials are essentially independent of the actual value of the modulation wave vector or the misfit between the two substructures. This contrasts with the conventional superstructure approach, where tiny changes of composition can imply a change in the space group symmetry and uncontrolled changes in the size of the superstructure unit cell, *i.e.* in the number of structural parameters.

In other words, the structural differences in these composition flexible systems caused by a composition variation can be quite drastic if described with conventional crystallography, while in the superspace description they can be explained and described by the change of the ratio γ (the modulation wave vector) keeping the rest of the structural model essentially unchanged. Under this premise, it is to be expected that the main structural features of all these $A_{1+x}[A',B]O_3$ materials can be described with an idealized single structural model in the superspace with the value of γ as a free parameter depending on the actual composition. The aim of the present paper is to propose a model of such type. The value of γ, and therefore the value of x, will be taken as arbitrary and therefore 'incommensurate' in the practical sense stressed above. It will be shown that the structural knowledge already available on compounds of the family together with some simple assumptions based on the layer model lead to a unique structural model in the superspace valid for any composition. The model does not only include the general structural features listed above, but has also additional predictive power. One can derive, for instance, general rules with respect to the sequences of octahedra and prisms in the columns (*i.e.* the stacking sequences of layers $[A_3A'O_6]$ and $[A_3O_9]$) as a function of the composition. In particular, it will be shown that these sequences are a generalization of that defined in the literature as the Fibonacci chain.[29]

2 The superspace description

The superspace formalism was introduced in the 1980s for the description of the so-called aperiodic crystals, *i.e.* incommensurate structures and quasicrystals,[30,31] but the usefulness of this approach for the description of normal structures as well, in particular superstructures, has become steadily clearer through multiple independent works.[26–28,32] In this section, we briefly summarize under this viewpoint the main concepts of this formalism. For simplicity and accuracy, we restrict the

discussion to modulated systems with a single modulation wave vector.

In general we can consider a structure as modulated along z according to a modulation wave vector $\boldsymbol{q}=\gamma\boldsymbol{c}^*$ if it can be described as a set of average atomic positions ($x_0{}^{\mu}$, $y_0{}^{\mu}$, $z_0{}^{\mu}$) ($\mu=1,..,s$) repeated periodically according to a Bravais lattice given by a unit cell with basis vectors $\boldsymbol{a}$, $\boldsymbol{b}$, $\boldsymbol{c}$, plus a set of periodic atomic modulation functions (AMF) $u_x{}^{\mu}(x_4)$, $u_y{}^{\mu}(x_4)$, $u_z{}^{\mu}(x_4)$, $p^{\mu}(x_4)$, of period 1, so that the fractional coordinates [$x^{\mu}(\boldsymbol{m})$, $y^{\mu}(\boldsymbol{m})$, $z^{\mu}(\boldsymbol{m})$] and occupation $p^{\mu}(\boldsymbol{m})$ of an atom μ in a cell $\boldsymbol{m}=m_1\boldsymbol{a}+m_2\boldsymbol{b}+m_3\boldsymbol{c}$ (where m_i is an integer), are cell dependent and given by:

$$x^{\mu}(\boldsymbol{m})=x_0{}^{\mu}+u_x{}^{\mu}[\gamma(m_3+z_0{}^{\mu})+\Phi] \quad (1)$$

$$y^{\mu}(\boldsymbol{m})=y_0{}^{\mu}+u_y{}^{\mu}[\gamma(m_3+z_0{}^{\mu})+\Phi] \quad (2)$$

$$z^{\mu}(\boldsymbol{m})=z_0{}^{\mu}+u_z{}^{\mu}[\gamma(m_3+z_0{}^{\mu})+\Phi] \quad (3)$$

$$p^{\mu}(\boldsymbol{m})=p^{\mu}[\gamma(m_3+z_0{}^{\mu})+\Phi] \quad (4)$$

where Φ is a particular initial value of the x_4 variable. The so-called four dimensional 'superspace' is then the result of 'adding' the fourth coordinate x_4 associated with the AMFs to the real space. In the superspace, under certain restrictions the expressions (1)–(4) can be given a geometrical meaning which is schematized using some examples in Fig. 4 and 5. The figures depict a projection on the plane (z, x_4) of a modulated structure with two atoms per average unit cell and average coordinates $z=0$ and $z=1/2$. The first atom with average position at $z=0$ has a displacive modulation, while the second at $z=1/2$ has only an occupational modulation described by a step function with full occupation limited to the interval indicated by a thicker line and vacant sites by crosses (Fig. 4 and 5).

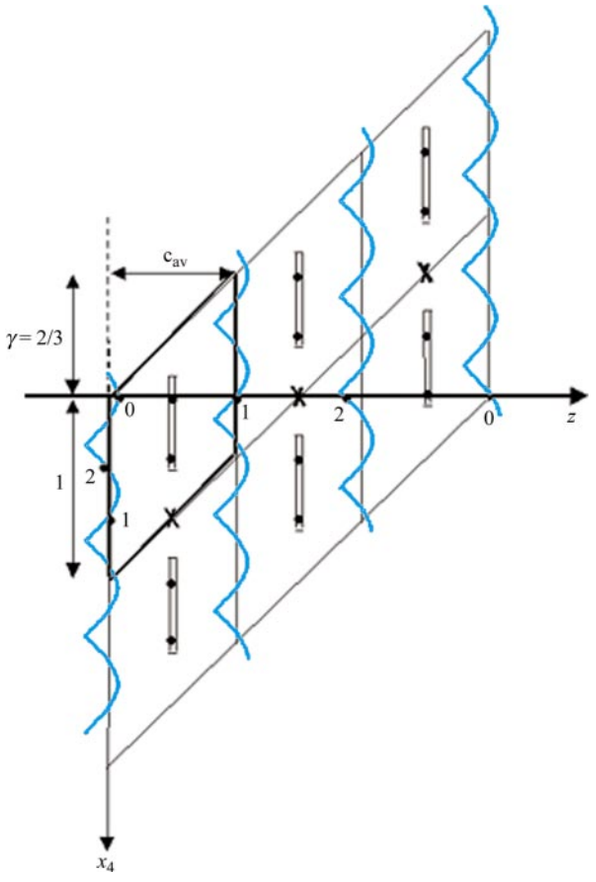

Fig. 4 Projection on the z/x_4 plane of the superspace description of a hypothetical modulated structure with two atoms per average unit cell and modulation wave vector $q=2/3c^*$ and initial phase $\Phi=0$. The points of the displacive modulation functions that are relevant on the three consecutive cells of the threefold superstructure are highlighted with filled dots numbered according to their order in consecutive average cells.

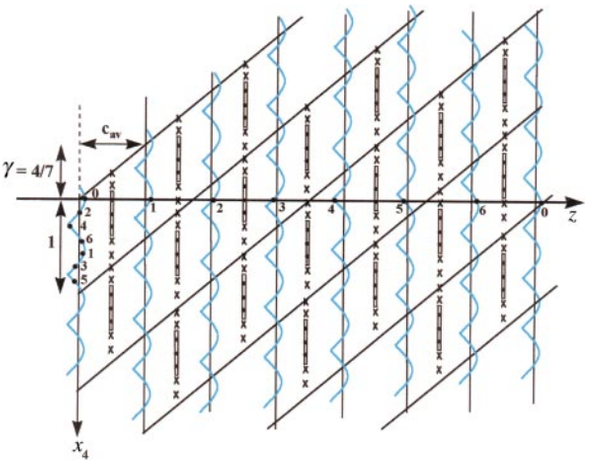

Fig. 5 The same superspace structure as in Fig. 4, but with modulation wave vector $q=4/7c^*$.

The continuous variable x_4 runs downwards along the vertical axis, while the horizontal one represents a projection of the real space along the z-direction. Similar schemes could be depicted for the equations corresponding to the coordinates x and y. Under this superspace construction, the real space structure can be interpreted as a section of a 4-dimensional periodic structure where the AMFs are represented along the 4th dimension. The value of the initial 'phase' Φ defines the section chosen. The superspace formalism recovers in this way the crystallographic concepts associated with periodic structures at the cost of having to work in a higher dimensional space. Fig. 4 depicts a hypothetical modulated configuration with wave vector exactly $(2/3)c^*$ and $\Phi=0$. Fig. 5 shows a structure with the same AMFs but with $\gamma=4/7$. In the first case, only three particular values within a period of each AMF are relevant as they are the only ones that appear periodically in the 'real' section z, producing a superstructure with $c_s=3c$. The actual value of Φ is especially relevant to define the three values of the AMFs which are realized in the real space structure. In Fig. 5, the period of the superstructure becomes $7c$, and consequently seven different values of each AMF (including vacancies from the step-like occupation AMF) are realized on the real structure. The initial phase Φ still plays a role here, defining the actual 'real space' points in the AMFs, but it is clear that as the supercell period becomes larger, the number of points in the functions which are physically realized increases correspondingly, and the Φ becomes less significant. In the mathematical limit of an infinite superstructure period (incommensurate q-vector) every point within a period of each AMF crosses once (and only once) the real section and the phase Φ becomes equivalent to an arbitrary choice of cell 'zero'. Hence, in general, the AMFs in the superspace description can be viewed as some kind of algebraic file of all the atomic positions (and occupations) in the crystal. In a commensurate superstructure this number is finite and Φ is a relevant parameter to define the corresponding points in the AMFs, while in the incommensurate case it is infinite and Φ is arbitrary. However, in both cases, the AMFs can be defined with a finite number of parameters, and the formal difference between both cases becomes irrelevant as the number of these parameters becomes significantly smaller than the number of atomic positions being described. For instance, if in Fig. 4 the value of γ were $2/3+\delta$ with δ close to zero, independently of the particular value of δ, rational or not, the whole AMF, instead of only three points, would become in practice relevant in the real structure. Notice that in this case the size of the interval

with non-zero occupation probability of the second atom is directly related to the composition of the material.

An important feature of the superspace description is that the set of all different chemical coordinations (up to any arbitrary distance) of a given atom species are also 'stored' along the fourth coordinate and easily retrieved by looking at different horizontal sections of the superspace construction. For instance, in Fig. 6, the different z-distances which happen between atoms in contiguous average cells for the case of Fig. 5 are indicated. Again an incommensurate $\boldsymbol{q}$-value would imply, instead of a discrete finite set of distances, that the whole continuous set of atomic distances given by the horizontal distance between the two AMFs for any value of x_4 are realized somewhere in the real structure.

The superspace description somehow separates the effect on the structure of the particular value of the modulation wave vector from the remaining structural parameters, in particular the parameters describing the AMFs. The AMFs are rather smooth functions or at least can be described with a small number of parameters. It can be seen with the example of Fig. 5 and 6 that a small change of the modulation wave vector while keeping the AMFs unchanged, can produce a drastic change of the supercell size but will scarcely vary the most immediate local environment of each atom. Only higher order coordination shells will suffer significant changes.

In general, the AMFs of a modulated structure with a single modulation wave vector satisfy symmetry properties described by a 4-dimensional superspace group.[30,33] In general, the existence of a symmetry operation $(\boldsymbol{R},\varepsilon\,|\boldsymbol{t},\tau)$ in the superspace symmetry group, implies:

(i) The operation $(\boldsymbol{R}|\boldsymbol{t})$ belongs to the (conventional) space group of the average structure given by the lattice vectors $\boldsymbol{m}$ and average fractional positions $({x_0}^{\mu}, {y_0}^{\mu}, {z_0}^{\mu})$.

(ii) The point group operation, described by the 3×3 matrix $\boldsymbol{R}$, must keep the direction of the modulation wave vector invariant, so that $\boldsymbol{Rq}=\pm\boldsymbol{q}$ (here we are assuming the modulation wave vector has not got an additional commensurate component along any direction).

(iii) If two atoms μ, ν are related by the operation $(\boldsymbol{R}|\boldsymbol{t})$ in the average structure so that atom μ is transformed into atom ν by the action of the operation $(\boldsymbol{R}|\boldsymbol{t})$, their corresponding AMFs are related according to the following relations:

$$\boldsymbol{u}^{\nu}(x_4)=R\boldsymbol{u}^{\mu}[\varepsilon(x_4-\tau)] \tag{5}$$

$$p^{\nu}(x_4)=p^{\mu}[\varepsilon(x_4-\tau)] \tag{6}$$

where $\boldsymbol{u}^{\nu}(x_4)=[{u_x}^{\nu}(x_4),\ {u_y}^{\nu}(x_4),\ {u_z}^{\nu}(x_4)]$ and $\varepsilon=+1$ or -1 depending on $\boldsymbol{Rq}=+\boldsymbol{q}$ or $-\boldsymbol{q}$. Eqns. (5) and (6) should be also satisfied if atoms $\boldsymbol{\nu}$ and $\boldsymbol{\mu}$ coincide, *i.e.* $(\boldsymbol{R}|\boldsymbol{t})$ keeps invariant atom $\boldsymbol{\mu}$ in the average position. In this particular case eqns. (5) and (6) with $\boldsymbol{\nu}=\boldsymbol{\mu}$ become a symmetry constraint on the form of the AMFs of atom $\boldsymbol{\mu}$.

In a commensurate case, the symmetry of the resulting superstructure can also be described by a normal space group which depends in general on the value of the initial phase Φ and can be derived from the superspace group.[26]

Let us consider now the example of a composite $X_{1+x}Y$ formed by two subsystems: one of Y atoms with a monoatomic average structure with cell c_1 along z, and the other formed by X atoms with average cell c_2 along z and two atoms per unit cell at average coordinates $z=1/4$ and 3/4. A possible embedding in the superspace (projection on the z, x_4 plane) of the structure of such a composite is shown in Fig. 7(a) for $x=0.2$. Again, the real structure (its projection along z) is given by the horizontal section. The geometrical construction ensures that the average positions of X(1) and X(2) atoms are repeated along z with periodicity c_2, while Y atoms have an average period c_1. The subsystem of Y atoms is depicted as a modulated structure with modulation wave vector $[(1+x)/2]c_1^*$ with the same embedding rules as in Fig. 4 and 5, while the modulated structure corresponding to the X atoms is shown in a distorted form. As in the single modulated structures depicted in Fig. 4 and 5, the AMFs of the X(1), X(2) and Y atoms can be considered a 'file' of all atomic positions realized in the modulated structure. Also all interatomic distances are stored along the coordinate x_4. The difference now is that the misfit between the two subsystems results in the distances between atoms belonging to different subsystem not being upper bounded, and the interatomic distances along z have also no lower boundary. If the system is incommensurate (x is irrational or, in practice, long period commensurate), the two subsystems can in principle 'slide' with respect to each other with negligible energy cost. This is the so-called phason degree of freedom and corresponds in the superspace scheme Fig. 7(a) to a change of the origin along x_4 and the corresponding change of the horizontal section that represents the structure in real space.

To use one or the other subsystem in a composite as a privileged reference, and hence described as a conventional modulated structure, is an arbitrary choice. For instance, an equivalent superspace embedding can be done, as shown in Fig. 7(b), with the subsystem X being the one depicted as a

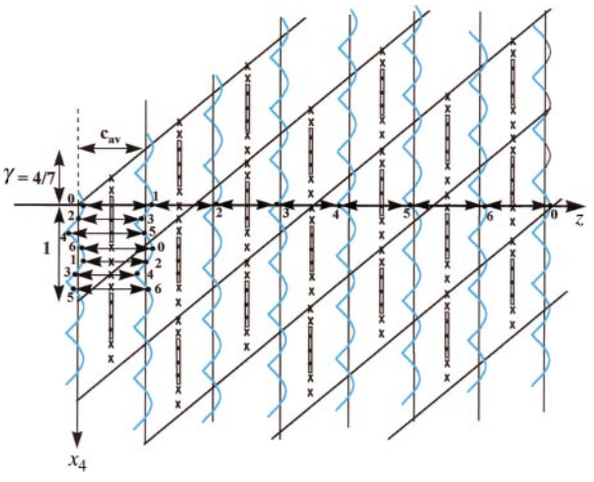

Fig. 6 The same zx_4 projection as in Fig. 5, showing how the different interatomic z-distances between atoms in contiguous cells can be retrieved from the relative positions of the modulations along x_4.

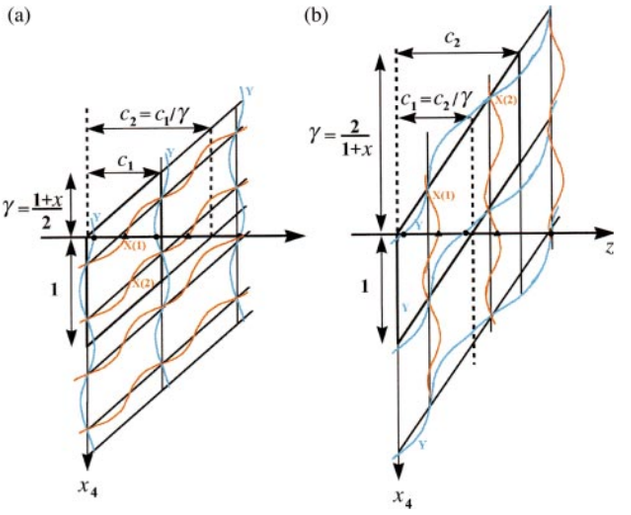

Fig. 7 (a) Projection on the zx_4 plane of the superspace description of a hypothetical composite $X_{1+x}Y$ modulated along the z-axis with $x=0.2$ and subsystem Y as reference. (b) The same structure as in (a), but with subsystem X as reference.

conventional modulated structure. The modulation wave vector is identified in this case with $\boldsymbol{c}_1^*$, so that $\boldsymbol{q}=\boldsymbol{c}_1^*=[2/(1+x)]\boldsymbol{c}_2^*$, and the metrics of the superspace unit cell is quite different from that in Fig. 7(a). However, the atomic positions along the section corresponding to the real z-axis of both figures coincide and, therefore, both representations are fully equivalent. One should stress that different choices of the superspace embedding imply in general a different definition for the fourth coordinate x_4, and consequently, also change the description of the superspace group, analogous to the changes of setting in normal space groups. In fact, in a composite the structural parameters of each subsystem are usually given using the superspace embedding where this particular subsystem is taken as reference, and therefore, in general, a different setting of the common superspace group is used for each subsystem.[27]

3 The subsystem [A′,B]O_3

Evain *et al.*[8] have recently analyzed the structure of $Sr_{1.2872}NiO_3$ as an incommensurate composite, and proposed as the symmetry of the compound the superspace group $R\bar{3}m(00\gamma)0s$ with subsystem NiO_3 as reference (see Table 1). We will start by assuming this superspace symmetry to be valid for the whole family of compounds, independent of the composition and actual atoms A, A′ and B involved in the compound. The assumption of a superspace group common to the whole family of materials directly introduces a restriction on the possible space group symmetries of the materials when described in conventional crystallography as 'superstructures'. As stressed above, the possible space groups of the resulting superstructures can be derived from the superspace group of the generic structure and depend in general on the value of the initial 'phase' Φ. For the superspace group $R\bar{3}m(00\gamma)0s$, this derivation has been carried out.[8] The results are reproduced in Table 2, with a slight correction concerning the possible special initial phases, and in a different form which emphasizes the equivalence of Φ values corresponding to different equivalent domains. According to Table 2, depending on the value of x (or γ) and the initial phase Φ, the symmetry can vary within a limited set of nine possible space groups. Typically, for a fixed composition, the space groups can be one of two or three depending on the value of Φ. This is a strong prediction coming from the model, and is in principle at variance with some of the symmetries proposed in the literature for some of the compounds.[21]

With $R\bar{3}m(00\gamma)0s$ as the superspace group of the subsystem [A′,B]O_3, the space group of its average structure must be $R\bar{3}m$. Also following the features of the above mentioned structure of $Sr_{1.2872}NiO_3$,[8] we take $Z=3$ in the average unit cell with the [A′,B] atom located at the origin, while the three oxygens are distributed on six half-occupied positions on the plane $z=1/2$ forming a hexagon which is symmetry-generated from a single independent position, for instance O(1) at $(x, x, 1/2)$. These six average oxygen positions can be separated into two types, oxygens O_a and O_b, forming two equilateral triangles, which correspond to the two possible orientations of the triangular O_3 faces on the [A′,B]O_3 columns (Fig. 8). The R-centering translations of the space group produce the two additional molecules in the average unit cell. The description of the actual

Table 1 Symmetry operations of the $R\bar{3}m(00\gamma)0s$ superspace group

$(E,1\|n_1n_2n_3n_4)$	$(\bar{1},\bar{1}\|0000)$
$(3_z^+,1\|0000)$	$(\bar{3}_z^+,\bar{1}\|0000)$
$(3_z^-,1\|0000)$	$(\bar{3}_z^-,\bar{1}\|0000)$
$(m_x,1\|000\frac{1}{2})$	$(2_x,\bar{1}\|000\frac{1}{2})$
$(m_y,1\|000\frac{1}{2})$	$(2_y,\bar{1}\|000\frac{1}{2})$
$(m_{xy},1\|000\frac{1}{2})$	$(2_{xy},\bar{1}\|000\frac{1}{2})$
$+(E,1\|\frac{1}{3}\ \frac{2}{3}\ \frac{2}{3}\ 0)$	$+(E,1\|\frac{2}{3}\ \frac{1}{3}\ \frac{1}{3}\ 0)$

Table 2 Possible space groups for commensurate structures with $q=\gamma c_1^*$ and superspace group $R\bar{3}m(00\gamma)0s$. For each, the necessary initial phase of the modulation Φ (see text) is indicated in sets of values corresponding to equivalent domains

$\gamma=p/k$			
$p=3n$	$\Phi=0$ (mod. $1/k$)	$\Phi=1/2k$ (mod. $1/k$)	$\Phi=$arbitrary
$k=$even	$R\bar{3}c$	$R\bar{3}c$	$R3c$
$p=3n$	$\Phi=0$ (mod. $1/2k$)	$\Phi=1/4$ (mod. $1/2k$)	$\Phi=$arbitrary
$k=$odd	$R\bar{3}$	$R32$	$R3$
$p\neq3n$	$\Phi=0$ (mod. $1/3k$)	$\Phi=1/6k$ (mod. $1/3k$)	$\Phi=$arbitrary
$k=$even	$P\bar{3}c$	$P\bar{3}c$	$P3c$
$p\neq3n$	$\Phi=0$ (mod. $1/6k$)	$\Phi=1/4$ (mod. $1/6k$)	$\Phi=$arbitrary
$k=$odd	$P\bar{3}$	$P32$	$P3$

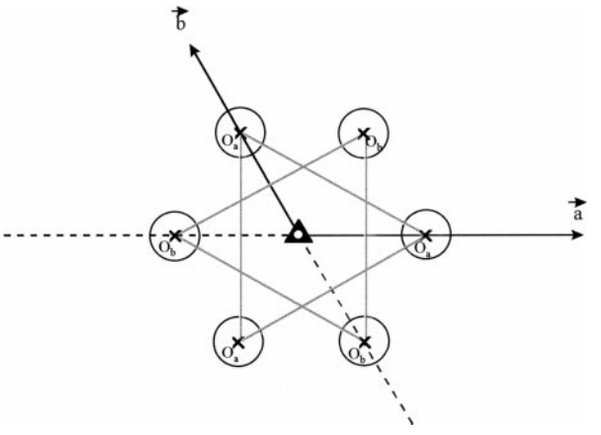

Fig. 8 Scheme of the average atomic positions of the oxygen atoms on the plane $z=1/2$ and centered around the origin. All positions are half occupied and the two distinct sets of atoms denoted O_a and O_b are indicated.

modulated structure is completed with the AMFs, both occupational and displacive, of the atoms in the asymmetric unit of the average structure, namely [A′,B] and O(1).

3.1 Occupation modulation functions

We will now show that the simplest choice of occupational AMFs for the single independent oxygen, compatible with the proposed superspace symmetry, leads directly to a simple x-dependent rule for the sequence of octahedra and prisms along the columns [A′,B]O_3 which is in agreement with the available observations.

The average oxygen at $(x, x, 1/2)$ (type O_a) is invariant for the operation $(2_{xy}|000)$, and therefore its AMFs should be invariant for the superspace group operation $(2_{xy},\bar{1}|000\frac{1}{2})$ [see Table 1 and eqns. (5) and (6)] :

$$p^{O_a}\left(-x_4+\frac{1}{2}\right)=p^{O_a}(x_4) \tag{7}$$

i.e. the function should be symmetric with respect to $x_4=1/4$ and 3/4. From eqns. (5) and (6) it is also easy to see that the occupational AMFs of the other two O_a atoms are identical and those of the O_b atoms are translated by 1/2 along x_4:

$$p^{O_b}(x_4)=p^{O_a}\left(x_4-\frac{1}{2}\right) \tag{8}$$

According to the structural features mentioned in the introduction, one can presume that the occupation of sites O_a and O_b is mutually exclusive, the sites being either fully occupied or empty. Under this assumption it is then easy to imagine the simplest AMF $p^{O_a}(x_4)$ compatible with the symmetry condition (7) and with the condition that on average $<p^{O_a}>=1/2$, that is the function:

$$p^{O_a}(x_4)=1 \quad 0<x_4<1/2 \tag{9}$$

$$p^{O_a}(x_4)=0 \quad 1/2<x_4<1 \tag{10}$$

Indeed, this is the occupational modulation of oxygen (a Crenel function) which has been proposed[8] for the compound $Sr_{1.2872}NiO_3$. Here we only want to stress that this form can be considered the simplest one compatible with the superspace symmetry and the empirical fact of the existence of triangular sets of atoms O_a and O_b separately along the columns. In Fig. 9, a scheme of these occupational AMFs in the superspace is shown. The figure has been constructed for a composition around $x=0.2$ ($\gamma=0.6$). One can easily see how the oxygens O_a and O_b are distributed along z forming a unique fully defined sequence with either consecutive triangles O_a–O_b or O_b–O_a (octahedra with the two distinct orientations), or consecutive O_a–O_a or O_b–O_b triangles (trigonal prisms with the two distinct orientations). If we assume now that all octahedra have B atoms inside and all prisms have A′ atoms inside, the form of the occupational AMFs for the 'average' atom [A′,B] is unequivocally determined and is also shown in Fig. 9. Let us note that the symmetry conditions (5) and (6) for this latter function (it should have periodicity 1/2 and be symmetric with respect to $x_4=0$ and 1/2) are satisfied automatically. Looking along the internal superspace coordinate x_4, the proportion of each polyhedron type on each column for an incommensurate case can now be seen. Consistent with the composition, we have a fraction $(1-x)/2$ of B atoms inside the O_a–O_b octahedra, and an equal fraction inside the O_b–O_a octahedra, while the A′ atoms can be within O_a–O_a and O_b–O_b prisms, a fraction $x/2$ in each situation. The distribution along x_4 of the different types of coordination follows the scheme in Fig. 10. For commensurate cases with $\gamma=p/k$, where k is odd, the equality of the number of prisms/octahedra with the two distinct orientations disappears, while it is maintained when k is even.

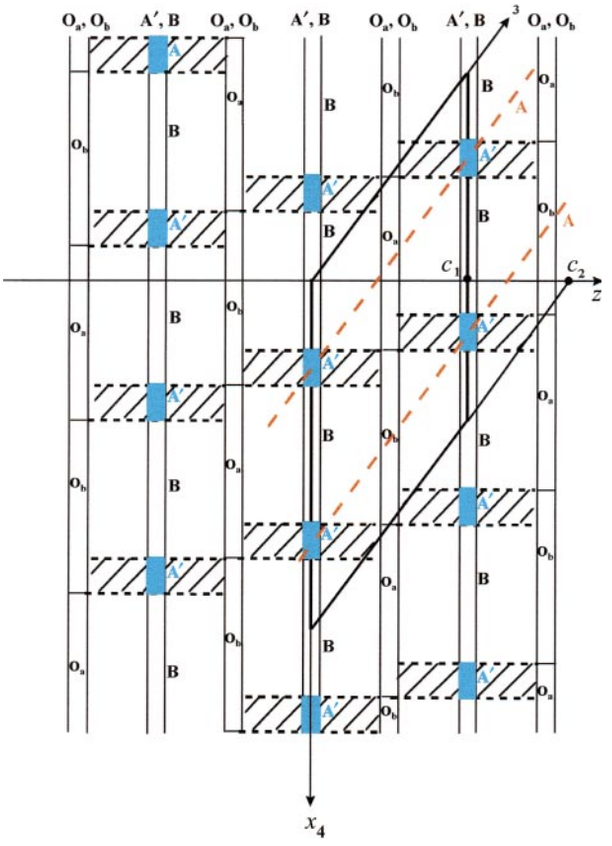

Fig. 9 Projection on the zx_4 plane ($\gamma=0.6$) of the occupational modulation functions of the subsystem $[A',B]O_3$, according to the model proposed. A unit cell is emphasized by thicker lines.

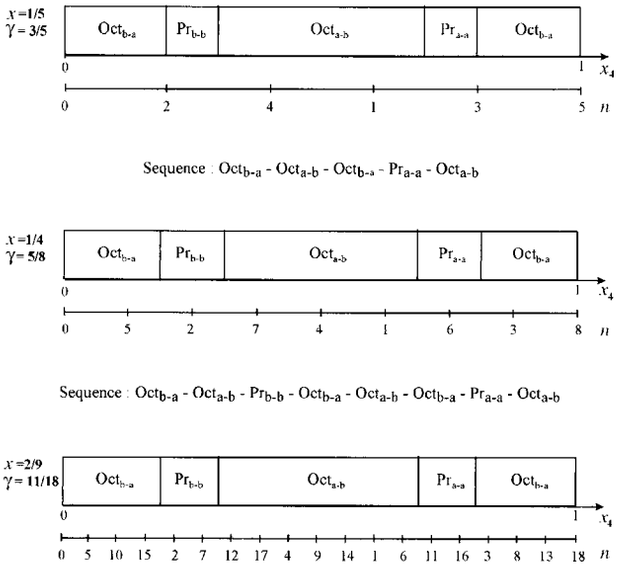

Fig. 10 Scheme of the O_6 configurations along the internal coordinate x_4 for a column of $[A',B]O_3$ resulting from the model in Fig. 9 for $x=1/5$, 1/4 and 2/9. The numbered discrete points correspond to the x_4 values ($\gamma n+\Phi$) associated with consecutive average cells along z. The resulting sequence of octahedra and prisms can be immediately derived and is indicated in each case.

3.2 The sequence of octahedra and prisms on the columns

Let us consider, for instance, the commensurate case $x=1/5$ ($\gamma=3/5$). According to eqns. (1)–(4), the values of the AMFs for the [A′,B] atom realized in the structure are consecutively those at $x_4=(3/5)n+\Phi$ with $n=0$, 1,..., 4. Hence, from the set of Crenel functions depicted in Fig. 9 and the scheme in Fig. 10, it is easy to derive that the sequence along the column is going to be 4 octahedra–1 prism. Depending on the initial phase this sequence is either (Oct_{a-b}–Oct_{b-a}–Oct_{a-b}–Oct_{b-a}–Pr_{a-a}) or (Oct_{b-a}–Oct_{a-b}–Oct_{b-a}–Oct_{a-b}–Pr_{b-b}). These two sequences are equivalent and could correspond to a twinning of the samples. If x is not exactly 1/5 but very close to it, it is straightforward to see from the superspace construction that the sequence along the column is going to be very similar. The periods of (4 Oct–1 Pr) will only suffer some 'fault' every few periods, the density of these faults being smaller the closer the value of x is to 1/5. Similarly, for $x=1/4$ ($\gamma=5/8$) it is straightforward to retrieve from the occupational AMF in the superspace that the sequence on the columns is (3 Oct–1 Pr), the period being 2 sequential units of the type (Oct_{a-b}–Oct_{b-a}–Oct_{a-b}–Pr_{b-b})–(Oct_{b-a}–Oct_{a-b}–Oct_{b-a}–Pr_{a-a}). The need for a second sequential unit in order to obtain a full period is obvious when seeing the sequence in terms of O_a and O_b layers, and results also from the denominator in γ that forces the relation $c_s=8c_1$. For all γ values with an even denominator the period will contain two equivalent sequential units, while for γ values with an odd denominator the period coincides with a single sequential unit and, as there are two equivalent configurations with distinct orientations, twinning with respect to these is then possible. It is worth mentioning that this is an additional twinning possibility which may occur whatever the tridimensional symmetry (P or R).

If one now considers the case $x=2/9$ ($\gamma=11/18$), and the resulting physical successive points $(11/18)n+\Phi_0$ ($n=0$, 1,..., 17) on the scheme in Fig. 10, it is straightforward to see that the sequence is (4 Oct–1 Pr–3 Oct–1 Pr), the period containing two sequential units. Hence the sequence is just the juxtaposition of the sequential units corresponding to $x=1/5$ and $x=1/4$. In general, from the general form of the occupational AMFs for the oxygens a general rule can be established which can be stated quite simply if the so-called Farey tree[34] is used (Fig. 11). Namely, if the value of x is n/m (where n and m are integers)

and in the Farey tree this fraction has as preceding 'generators' the fractions n_1/m_1 and n_2/m_2, so that $n/m=(n_1+n_2)/(m_1+m_2)$, the sequence of octahedra and prisms on the columns will be just the juxtaposition of the sequences corresponding to the x-values n_1/m_1 and n_2/m_2. If this rule is followed systematically starting with the simplest fractions $x=0/1$ (1 Oct) and $x=1/2$ (1 Oct–1 Pr), the sequence for any arbitrary composition can be derived. For irrational values of x, the corresponding aperiodic sequence can be approximated through successive fractions approaching the actual value of x up to any desired accuracy.

Therefore, according to the above general model, for a given composition x there is only one possible sequence. This result can be compared with the sequences predicted[21] with plausible layer arrangements. In all cases a unique sequence is proposed which coincides with that obtained from the general rule stated above. For complex cases, such as $x=2/5$, 2/7 or 5/13, for which these authors consider two sequences as plausible only one of them corresponds to that deducible from the Farey tree rule. To the best of our knowledge, all sequences observed experimentally are also consistent with this rule, and therefore with the general model we are proposing.

These sequences of octahedra and prisms along the columns can be compared with the so-called Fibonacci chain introduced in the analysis of quasicrystals as one of the simplest models of quasiperiodicity.[29] The Fibonacci chain is a mathematical sequence of two different segments S and L (short and long, respectively) along a single direction with a relative ratio between the number of intervals S and L equal to the golden mean $\tau=(\sqrt{5}-1)/2=0.618034$, so that the 'composition' of the chain can be expressed with the formula S_xL_{1-x} with $x=\tau/(1+\tau)=1-\tau=0.381966$. The aperiodic Fibonacci sequence can be constructed making use of the Farey tree and the same rule explained above particularized for successive fractions approaching the irrational value $x=1-\tau$ up to any desired accuracy. If we identify the segments S and L with the prisms and octahedra, respectively, their sequences in the columns of $(A'_xB_{1-x})O_3$ can be then considered a generalization of the Fibonacci sequence for an arbitrary relative composition of the two segments. Hence, $A_{1+x}(A'_xB_{1-x})O_3$ compounds may produce a physical realization of the Fibonacci chain if their composition is 'tuned' to the necessary value $x=1-\tau$. This property may be of particular importance considering that the physical properties of the Fibonacci chain, as a prototype of one-dimensional quasiperiodic systems, have been extensively studied from a theoretical viewpoint. Materials of a family with the appropriate composition could then be used as an experimental benchmark for such studies, for instance with respect to electronic and magnetic properties. Let us note that the octahedra are in general shorter along z than the prisms; this means that when compared with the usual representation of a Fibonacci chain, we are reversing the length of the L and S units, so that L is the shortest. This change is irrelevant from a physical viewpoint. A second more important difference is the fact that two types of prisms and octahedra exist on the columns (prisms Pr_{a-a} and Pr_{b-b}, octahedra Oct_{a-b} and Oct_{b-a}) depending on the oxygen triangles involved. If these differences are taken into account, some additional complexity with respect to the theoretical Fibonacci chain is present in the columns and causes the modulation wave vector to be $(1+x)/2$ instead of $x/2$. Thus, for a composition $x=1-\tau=0.381966$ which yields (approximately) the Fibonacci sequence of prisms and octahedra along the column, the modulation wave vector is not τ but $(2-\tau)/2=0.690983$.

Fig. 9 permits us not only to distinguish clearly the sequence of octahedra and prisms along the columns but also, for a fixed value of x_4 which particularizes a certain octahedron or prism in the column, one can observe by just looking at its neighborhood along z the existing neighbors above and below along the column. Thus, one can easily deduce for instance that all prisms are isolated, *i.e.* bordered by an octahedron above and below (along z). Also, one sees that a fraction $x/(1-x)$ of all the octahedra have neighboring prisms above and an equal fraction have a neighboring prism below. Octahedra limited by prisms both above and below will occur if $x>1/3$, and the fraction of octahedra in this situation will be $(3x-1)/(1-x)$. At the limit $x=1/2$, all octahedra are limited by prisms on both sides.

Up to now we have only analyzed the distribution of prisms

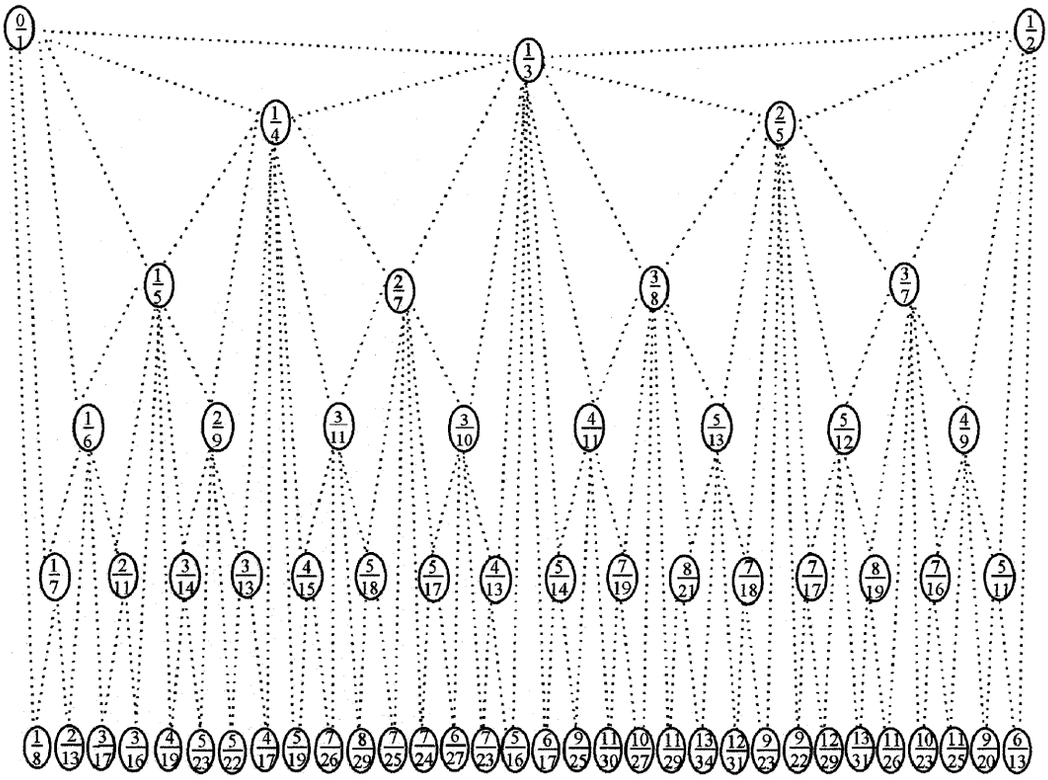

Fig. 11 Scheme of the Farey tree within the interval [0, 1/2].

and octahedra along the column centered at the origin of the plane xy, however, there are two other columns to be considered in the average unit cell, which are derived from the first through the action of the R-centering superspace translations (1/3, 2/3, 2/3) and (2/3, 1/3, 1/3). The three columns are centered at the points (0,0), (1/3, 2/3) and (2/3, 1/3) on the plane xy, so that they can be viewed as occupying the vertices of an equilateral triangle, the A(1) cations being located at their interstice. In Fig. 12, the projection on the plane zx_4 of the occupational AMFs of the oxygens of the three columns is shown. Taking the viewpoint of the A cations located between the three columns, it is interesting to see that the shift of the common sequence of octahedra and prisms from one column to another causes the trigonal prisms along z in the three columns around to be distributed as uniformly as possible.

3.3 Displacive z-component modulation functions

The oxygen positions are not only modulated with respect to their occupation, but also must have some x_4-dependent displacement that will distinguish the prismatic and octahedral sites. The approximate form of the AMFs along z can be easily imagined. Again, the simplest situation compatible with the superspace symmetry and the geometric requirements is quite obvious. If we make the approximation that all prisms and octahedra are geometrically equivalent so that they all have the same length along z, D_p and D_o respectively, it implies that all distances along z between consecutive triangles O_a–O_a, O_b–O_b in the trigonal regions should be equal to D_p, while the common value for any z-distance between pairs of triangles O_a–O_b and O_b–O_a should be D_o. This can only be achieved with a sawtooth modulation for the oxygens as depicted in Fig. 13. The function is antisymmetric with respect to the points $x_4=0.25$ and 0.75, as required by the superspace operation $(2_{xy}, \bar{1}|000\frac{1}{2})$. As expected from the analogy above, the scheme of the oxygen modulation is quite similar to the superspace (modulated) representation of a Fibonacci chain to be found in the literature.[35] In contrast, with it, the existence of two different oxygen types introduces an additional doubling of the period along the internal space, while the oblique angle in the superspace unit cell that defines the modulation wave vector is composition dependent and not restricted to any particular value.

If the atoms B and A′ are always imagined to be located at the centers of the octahedra and prisms, respectively, they also must have a sawtooth modulation along z, as shown in Fig. 13. If this sawtooth modulation of the cations B and A′ did not exist, it would imply in fact that the position of these cations would be modulated when seen relative to their surrounding oxygens. The sawtooth functions related to the cations B and A′ are respectively defined by $\delta_B=(1-x)\delta_O$ and $\delta_{A'}=x\delta_O$. It is important to point out that the set of AMFs proposed in Fig. 13 for describing the columns $(A'_xB_{1-x})O_3$ only includes a single free parameter, namely the semi-difference between the z-lengths of the prisms and octahedra, $(D_p-D_o)/2$, henceforth denoted δ_O.

If δ_O is assumed to be composition independent, a linear relation between the average cell parameter c_1 and x can be easily derived from the geometric construction of Fig. 13: $c_1=D_o+2\delta_O x$ which is merely equivalent to the simple and

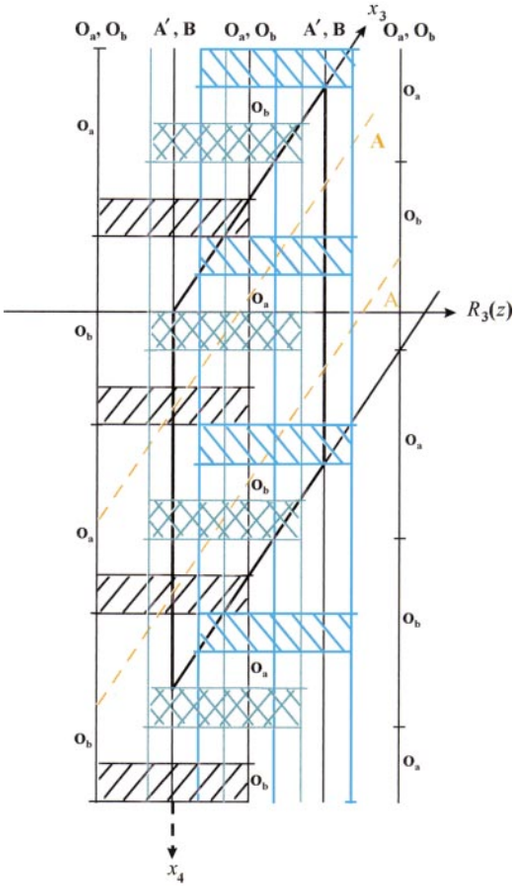

Fig. 12 Projection on the zx_4 plane of the existence lines (average position) of three neighboring $[A',B]O_3$ columns related by the R-centering translations. The regions along x_4 with prismatic coordination are emphasized. The existence lines of the A(1) and A(2) atoms are also depicted.

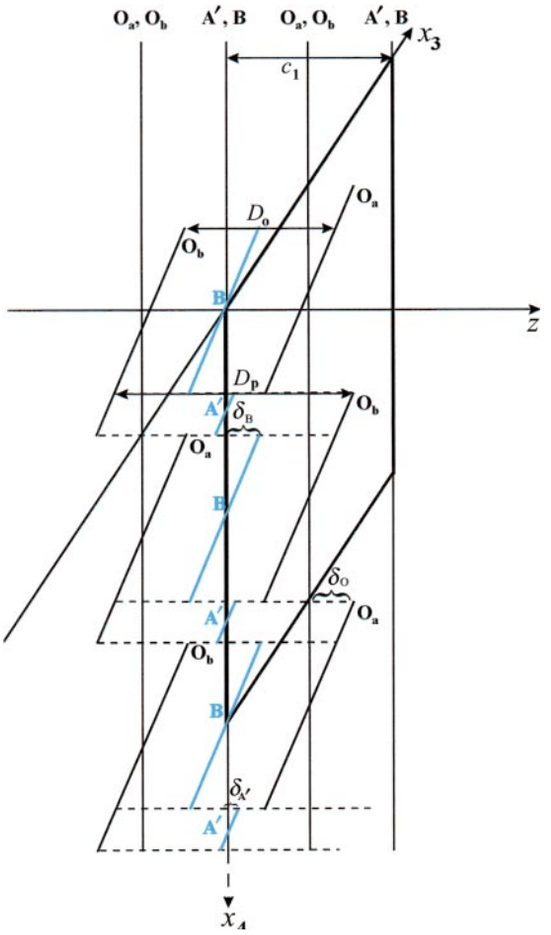

Fig. 13 Projection on the zx_4 plane ($\gamma=0.6$) of the displacive modulation functions of the subsystem $[A',B]O_3$ according to the model proposed. A unit cell is emphasized by thicker lines. The sawtooth structure of all the functions is described by the single parameter δ_O.

quite logical statement that c_1 should be the average of the distances D_p and D_o according to their relative frequency along the column, *i.e.* $c_1=(1-x)D_o+xD_p$. This relation can be confirmed in the series of compounds Ba_{1+x}[Cu,Ir]O_3 which have recently been characterized.[4,21] Fig. 14 shows the clear linear correlation of c_1 and x for the five reported compounds, all with x within the interval [0.2, 0.3]. The linear fit gives the values 2.57 and 0.56 Å for D_o and $2\delta_O$, respectively. These values compare fairly well with the average metal–metal distance within contiguous octahedra of 2.56 Å derived for the structure of $Ba_6CuIr_4O_{15}$ ($x=0.2$)[4] and in contiguous octahedra and prisms (2.91 Å) for the same structure, which would correspond to a $2\delta_O$ value of 0.68 Å.

The modulation model of Fig. 13 can be compared with the structure of $Sr_{1.2872}NiO_3$.[8] The z-component AMFs for the atoms in a single column of this structure are reproduced in Fig. 15. The oxygens follow the scheme of sawtooth functions. This feature is more remarkable if we take into account the fact that the functions were parameterized using a Fourier-type basis of functions whose amplitudes were the parameters adjusted in the refinement.[8] From the figures one can estimate $\delta_O=0.35$ Å; from this value and with $x=0.287$ and $c_1=2.574$ Å for this compound the values of D_o and D_p can then be easily derived as 2.37 and 3.07, respectively. To compare the modulation of the Ni cations it is important to take into account that, according to the structural model of ref. 8 the Ni sites at the prisms are split in the average unit cell and populate some split positions around the center of the prisms, both on the column axis and also at the centers of the rectangular prism faces. In the prismatic regions, Fig. 15 only depicts the modulation of the partially occupied Ni site located at the center of the prism faces, which is the only prismatic Ni site which is modulated in the model. It can be clearly seen that the determined modulations comply approximately with the model in Fig. 13. They are also sawtooth modulated, as expected, so that the Ni is always equidistant from the two contiguous triangular oxygen layers. In the case of the Ni atoms with octahedral coordination, a clear deviation from this scheme can be observed. This feature is quite significant as is also observed in the commensurate model which was obtained independently in a conventional superstructure approximation, when described in the superspace (see Fig. 15). The sawtooth function flattens as it approaches its boundaries indicating that the Ni becomes acentric at the corresponding octahedra. If we consider the scheme in Fig. 9, and taking into account that for this compound $x/2=0.15$, one sees that most of the octahedral Ni cations have a contiguous prism, either above or below, so that their oxygen coordination is acentric with respect to second neighbors along the chain. This contrasts with the Ni atoms at the prism faces which have neighboring octahedra on both sides along z, and thus have a rather symmetric coordination up to second neighbors. This may be the

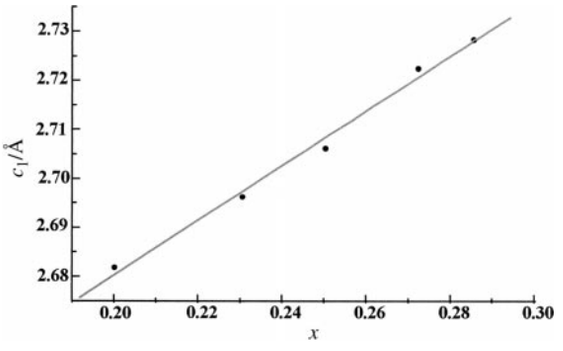

Fig. 14 Experimental parameter c_1 as a function of the composition x of different compounds[4,21] of the type Ba_{1+x}[Cu,Ir]O_3 and the linear fit corresponding to the law $c_1=D_O+2\delta_O x$.

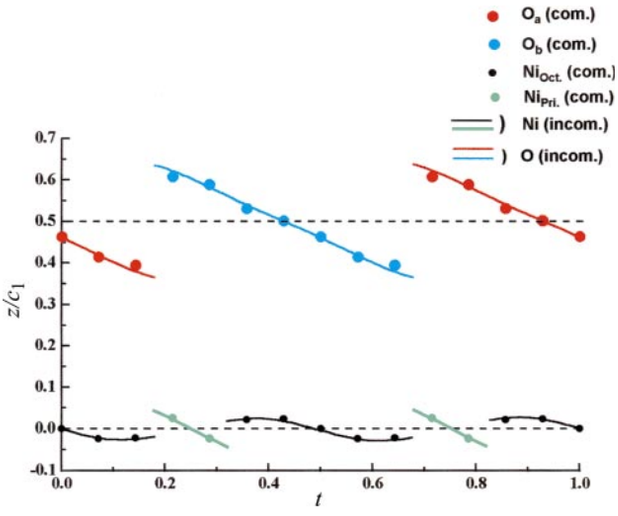

Fig. 15 Graphical representation of z/c_1 *versus* x_4 of the structure of the subsystem NiO_3 in the compound $Sr_{1.2872}NiO_3$.[8] Modulations are viewed along the shifted internal coordinate $t=x_4+qr_{av}$, which is coincident with the x_4 coordinate for the Ni atoms. The discrete points indicate the set of atomic positions corresponding to the alternative commensurate structural model proposed.[8]

explanation for the flattening of the modulation of octahedral Ni: the cation somehow gets closer to the oxygens of the contiguous prism. Only about 20% of the octahedral Ni atoms, those close to the points $x_4=0$ and 1/5, also have contiguous octahedra both above and below, and it is just at this point that the AMF approaches ideal sawtooth behaviour. Hence, we can speculate that in general the AMFs along z of the octahedral B cations will become closer to the sawtooth model the smaller the value of x.

Obviously, any accurate experimental determination of the structure of a single compound will deviate somehow from it. However, it is the natural reference for the description of any structure within the family and for its comparison with the structures of other compounds. It is also, in principle, the best starting point for a refinement process of experimental diffraction data. For instance, in the structural model discussed above,[8] the split Ni positions at the prism centers were left unmodulated, presumably to keep the number of adjustable parameters in the refinement under reasonable limits. But from the discussion above it is clear that keeping these Ni positions unmodulated paradoxically introduces an unwanted modulation of their positions relative to neighboring oxygens along z, which, in general, can be considered an artifact. A Ni position at the centers of the prisms in the starting model requires, in general, the presence of a sawtooth modulation fully correlated with that of the oxygen, as shown in Fig. 13.

3.4 Displacive *xy* modulation functions

According to eqns. (5) and (6), the superspace symmetry forbids the modulation on the xy plane of the atoms A′ and B, as their average position is at the origin. On the other hand, the superspace symmetry restrictions for the xy modulations of the oxygens [eqn. (5) and (6)] imply that the trigonal symmetry of the O_3 triangles forming the bases of both prisms and octahedra is always kept, while they can rotate and 'breathe' along x_4 (and therefore along z). This modulation should follow a helicoidal pattern. It is interesting that the invariance of the representative oxygen with respect to the symmetry operation $(2_{xy}, \bar{1}|000\frac{1}{2})$ forces this pattern to have a symmetry line along the direction (1, 1) on the plane xy at the points $x_4=1/4$ and 3/4, where the modulation cannot have a rotation component and should be limited to an eventual breathing. These points correspond to the centers of the octahedral regions of the modulation of [A′,B] along x_4. Except for these

symmetry-forced features, we have no steric or plausibility argument for postulating a particular form for these functions. In general, one can expect they will be quite small compared with the modulations along z, and they can be neglected in the idealized model we are discussing.

4 The subsystem A

The average unit cell of the second subsystem is not R-centered as with the $[A',B]O_3$ subsystem, but primitive. The reason is that the R-centering superspace operations $(1,1|\frac{1}{3}\frac{2}{3}\frac{2}{3}0)$, $(1,1|\frac{2}{3}\frac{1}{3}\frac{1}{3}0)$ in the setting of the $[A',B]O_3$ subsystem, become $(1,1|\frac{1}{3}\frac{2}{3}0\frac{2}{3})$ and $(1,1|\frac{2}{3}\frac{1}{3}0\frac{1}{3})$, respectively, in the setting with subsystem A privileged, where the role of components z and x_4 must be interchanged. This means that the average structure of this second subsystem formed by the cations A has additional lattice translations, $(\frac{1}{3}\frac{2}{3}0)$ and $(\frac{2}{3}\frac{1}{3}0)$, on the xy plane, and a primitive average unit cell can be chosen with $(\frac{1}{3}\frac{2}{3}0)$ and $(\frac{1}{3}\bar{\frac{1}{3}}0)$ as unit cell vectors on the xy plane. This primitive average unit cell contains two cations A(1) and A(2) at $(1/3,0,1/4)$ and $(2/3,0,3/4)$, respectively (only one symmetry-independent). Therefore, in the setting with subsystem $[A',B]O_3$ as reference, which we have used up to now, the superspace lines describing the average position of atoms A neglecting modulations (*i.e.* the 'existence' lines of these atoms) follow the scheme in Fig. 7(a). Note that the average c-unit cell parameter to which the z-coordinates of the A cations refer is now c_2 instead of c_1. The misfit between the c-parameters of the two subsystems makes possible that A cations are found along z at any height with respect to the [A′,B] atoms on the columns. Fig. 12 shows the beautiful correlation of the modulation on the $[A',B]O_3$ columns (*i.e.* the presence of trigonal prisms and A′ instead of B atoms) with the relative positions of the A cations of the second subsystem. The existence lines of the A cations cross the existence lines of the [A′,B] atoms of the three surrounding columns just at the centers of the 'prismatic regions'. This means in real space that prisms and A′ cations are located along the columns at the points where a neighboring A cation has its z-level considerably shifted with respect to the oxygen layers of any of the surrounding columns and approaches the height corresponding to the midpoint between two oxygen triangles along the column. In other words, in contrast with other types of modulated composites, the two subsystems are strongly correlated and the occupational modulation of the [A′,B] cations is an efficient way for getting the A′ atoms and the excess A cations close together over the whole structure.

Incidentally, in the case of an incommensurate (or long period) composite, the strong modulation of the $[A',B]O_3$ subsystem producing the O_6 prisms along the columns and its coupling with the subsystem of A atoms is bound to freeze the phason-like sliding of the two subsystems, usually present in incommensurate composites. A dynamic phason in these compounds would necessarily produce the interchange of B and A′ atoms, as the prisms should follow the z-sliding of the neighboring A cation. The obvious energetic barriers for such discrete structural changes makes certain the non-existence in these systems of a conventional phason branch. Only in the cases where A′ and B atoms coincide, the difference presumably being their oxidation state, phason-like relaxational dynamics can be envisaged which, similarly as occurs in quasicrystals,[36] could involve discrete flips of oxygen triangles from configuration O_a into O_b, and *vice versa*. However, a rather peculiar additional feature of the eventual phason flips in these materials would be the correlated presumed valence 'switch' of the B cations in order to transform from octahedral tetravalent cations into divalent prismatic ones.

A more complete perspective of the correlation between the subsystem of the A atoms and columns is obtained if we also take into account the relative position of the z-component AMFs of the oxygens in the three columns surrounding a set of A atoms, as depicted in Fig. 16 for $x=0.25$. We have chosen in this graphical example a case with $x\neq0.20$ to avoid the peculiarity of this particular value with respect to the functions of the A cations (see below) and to show the general validity of the argument. The lines of existence of the A cations not only cross the centers of the three prismatic regions for the existence lines of the [A′,B] atoms in the three columns, but also the centers of the oxygen sawtooth functions in the octahedral regions. Thus, the shift along z of the three columns produced by the R-centering is such that the z-level of the oxygens in the three columns is regularly shifted from one column to another, so that the A cation is rather close to the oxygen triangle in one of the surrounding columns. Then, two types of situations can be distinguished for the z-level of the average position of atom A: (i) it is close to the center of a prism in one of the surrounding columns and (ii) it is closer to the z-level of a triangle of oxygens in one of the surrounding columns. These regions alternate up to three times along the existence line of the A cation, corresponding to the three neighboring columns.

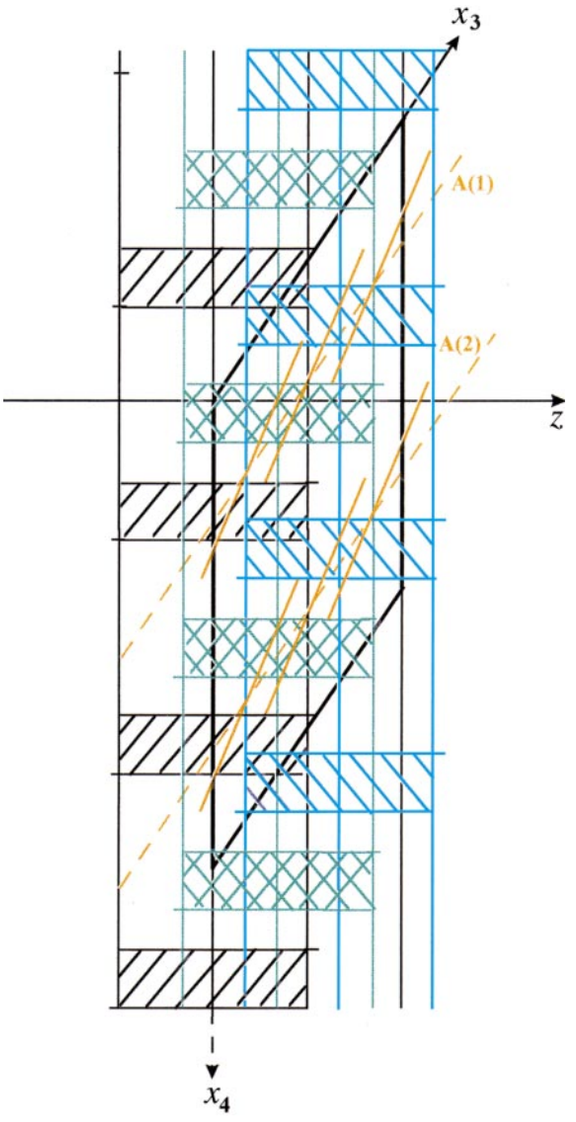

Fig. 16 Projection on the zx_4 plane of the displacive z-component sawtooth functions (full lines) corresponding to the oxygens of three neighboring columns $[A',B]O_3$ related by the R-centering translations according to the model proposed for $x=0.25$. Only the functions relevant to describe the environment of the A(1) and A(2) cations are indicated. The regions with prismatic coordination for each column along x_4 are also emphasized. The dotted lines correspond to the average positions (existence lines) of these atoms.

Up to now we have only discussed the average positions of the A atoms repeated with periodicity c_2 along z and their relative z-position with respect to the atoms in the subsystem of $[A',B]O_3$ columns, since this is, in fact, what the so-called existence line of the A atoms in Fig. 16 depicts. But A atoms should also be modulated as a result of their coupling with the columns. The layer model[1] mentioned in the introduction helps us to guess a first approximation of the corresponding z-component AMFs. According to the layer model (see Fig. 1), the A atoms are located at the level of the centers of the prisms, if present, and at the level of the oxygen triangles in the other columns. In a real compound, these two properties cannot in general be achieved simultaneously because the z-length of the prisms is not double that of the octahedra, as assumed by the model. We can however relax the restriction and presume that A atoms will tend to fulfill either one of the two conditions, as seen in short period compounds of the family, or satisfy some compromise between them. Indeed, we have already seen that the structure, and in particular its symmetry (the R-centering), seem to have the specific aim of situating the average positions of A atoms as close as possible to either one or the other condition. We can therefore imagine an A z-modulation which tries to complete the process, *i.e.* the modulation will deviate the z-coordinate of the A atom from its average position (the 'existence' line) so that it acquires the same height as either the center of the neighboring prism, if existing, or if not, the neighboring oxygen triangle. The hypothetical modulation is depicted in Fig. 17(a) for $x=0.2$ in the setting of the first subsystem. A clearer picture of the situation can be obtained if the subsystem of A atoms is regarded in the second setting with subsystem A as the reference modulated structure, as in Fig. 7(b). Fig. 17(b) depicts the modulation along the new internal coordinate, x'_4, running along the horizontal axis, which corresponds to the oblique direction of the existence line of A(1) in Fig. 17(a). One can see that the function is again a sawtooth function with two distinct intervals corresponding to the subsequent prismatic and octahedral x'_4 regions. The period 1/3 of the function and its antisymmetry with respect to 0, 1/6, 2/6..., 5/6 is forced by the superspace symmetry operations $(2_x\bar{1}|00\frac{1}{2}0)$, $(3_z^+,\bar{1}|\frac{1}{3}\frac{2}{3}0\frac{2}{3})$ and $(3_z^+,\bar{1}|\frac{2}{3}\frac{1}{3}0\frac{1}{3})$ [eqns. (5) and (6)] which keep the average position of A(1) invariant [eqns. (5) and (6)]. These symmetry features are fully consistent with the sawtooth function proposed. The prismatic and octahedral intervals are $x/(1+x)$ and $(1/3)-[x/(1+x)]$, respectively, so that the two intervals always sum a period 1/3 of the function, and at the limit $x=1/2$, the octahedral intervals (z-levels with no prism on any of the three surrounding columns) disappear. Both sawtooth functions always have the same slope, which can be easily derived from the geometrical construction; its value is $[D_o-2\delta_o]$ $(=[2D_o-D_p])$, so that the values $\delta_A{}^p$ and $\delta_A{}^o$, defining the sawtooth amplitudes in each interval, satisfy the relation $\delta_A{}^p+\delta_A{}^o=[D_o-2\delta_O]/2$ with $\delta_A{}^p/\delta_A{}^o=3x/(1-2x)$, so that $\delta_A{}^p=[x/2(1+x)][D_o-2\delta_O]$. Notice that for $x=0.2$ both octahedral and prismatic intervals have equal widths and the maximal displacement of the two sawtooth functions with respect to the average position of A(1) is minimized for this composition.

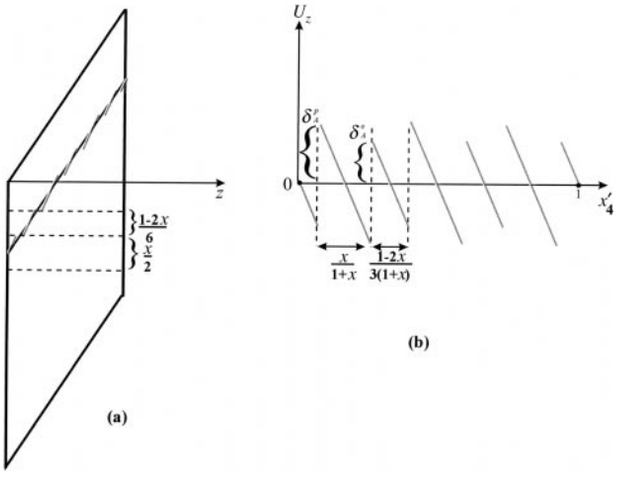

Fig. 17 (a) Hypothetical ideal displacive z-modulation ($\gamma=5/8$) of the A(1) cations ($z=1/4$) seen in the setting with subsystem $[A',B]O_3$ privileged. (b) The same modulation along the internal coordinate in the setting with subsystem A privileged.

The modulation functions of A(1) cations proposed in the scheme in Fig. 17(b) are much more speculative that those of the first subsystem, since in this case no stereochemical argument somehow forcing the form of the function exists. The proposed sawtooth functions are only the result of assuming, following the layer model, that the A cations should be located either at the level of the prism centers or at the level of the oxygen faces of the octahedra. The actual modulation in real systems may be a much smoother function with some kind of compromise between both roles. In any case, the function in Fig. 17(b) can be interpreted as a scheme of the z-distances, with respect to the average position of cation A(1), of the neighboring prism centers and the closest octahedral O_3 triangles. Under this viewpoint, the composition $x=0.2$ seems to have special significance. For this composition these z-distances in both prismatic and octahedral intervals are minimized and this would also be approximately true for any composition around this value, so one may speculate that incommensurate compositions around $x=0.2$ may be easier to synthesize than those approaching the two extreme limits $x=0$ and 1/2.

A comparison of the function in Fig. 17(b) with the modulation in a real system would clearly indicate the degree of correlation between the z-coordinate of the A cations and the local structure of the three neighboring $[A',B]O_3$ columns. This can again be done with the structural models (both commensurate and incommensurate) proposed for $Sr_{1.2872}NiO_3$[8] which are shown in Fig. 18 superposed with the theoretical sawtooth model. The correlation is quite striking for the sinusoidal modulation of the incommensurate model. The fitted value of the single Fourier amplitude used in the parameterization of the refined function seems to be optimal to mimic the suggested sawtooth behavior. One can see from this result that a sawtooth starting model can be much better adapted for an optimal refinement of the structure. The discrete points in the figure correspond to the alternative commensurate model ($x=2/7$), also refined in ref. 8. Unfortunately, in contrast with the case of the first subsystem, here the commensurate discrete positions clearly deviate from those suggested by the incommensurate model when particularized for $x=2/7$. The difference is rather significant; 0.1 Å displacements compared with 0.02 Å in the commensurate model. The reason for this inconsistency between the two models is unclear, but the coincidence of the discrete positions suggested by the incommensurate model with the z-level of the prism centers, as represented by the sawtooth function, suggests that the latter may be closer to reality.

5 The layer model

The structural model worked out above can be considered a 4D superspace derivation of the layer model[1] if relaxed from the condition $D_p=2D_o$ that is forced if layers are considered strictly rigid. The deviation of the structure above from this rigid layer picture can be clearly seen in Fig. 16, where the intersections of the three oxygen sawtooth functions with the z-real axis at $x_4=0$ indicate the different z-levels of the oxygens in the three neighboring columns, which a rigid layer model will situate on the same z-level. Indeed, it is enough to add to the

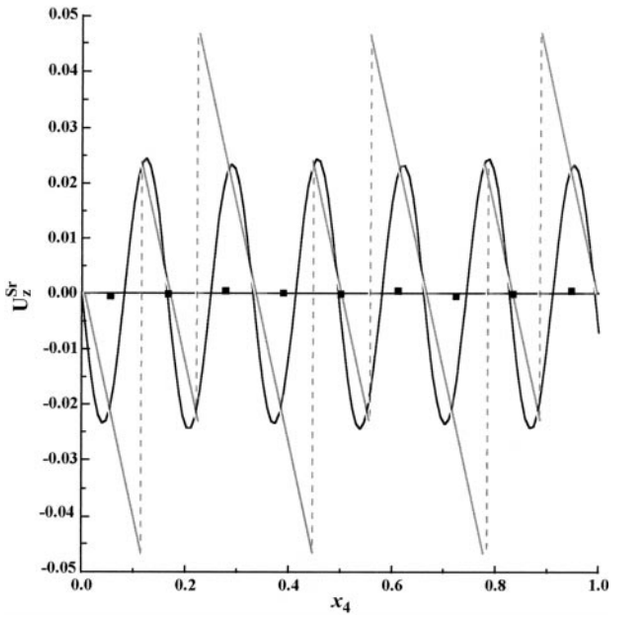

Fig. 18 Graphical representation of the displacive z-component modulation of the Sr cations in the compound $Sr_{1.2872}NiO_3$.[8] The discrete points indicate the set of atomic positions corresponding to the alternative commensurate structural model.[8] For comparison the model sawtooth modulation [see Fig. 17(b)] resulting from the empirical values of D_o and δ_O (see Fig. 15) for this compound is also shown.

above 4D composite structural model the additional layer condition $D_p = 2D_o$ for the slope of the three sawtooth functions. This particular value makes the three functions superpose so that the oxygens on the three columns are at the same z-level forming a layer. Thus, the z-misfits of oxygens in different columns are a natural consequence of the deviations of the O_6 prisms from their 'layer' size, and should be taken into account in any realistic model. The merging into the rigid layer model when $D_p = 2D_o$ can also be seen on the general modulation for cation A(1) suggested in Fig. 17. The slope $[2D_o - D_p]$ of the sawtooth functions becomes zero, meaning that the A cations require no modulation for being at the same level of the oxygens and prism centers. In fact, the existence lines of these cations which describe their average position superpose, in this case, with the sawtooth functions describing the modulation of oxygens and prism centers.

It is also interesting to compare the expressions for the superstructure cell parameter c_s as a function of the average thickness of the layers, e, and the integers m and n in the formula $A_{3n+3m}A'_nB_{3m+n}O_{9m+6n}$, which were derived in the introduction under the layer model, with the exact ones coming from the value of γ. For $\gamma = p/k$, where p and k are integers, we have $c_S = kc_1 = pc_2$. The value of γ expressed as a function of n and m is $[3(n+m)]/[2(2n+3m)]$. Considering that n and m are mutually prime, it is then easy to arrive rigorously at the same expressions for c_s as in the introduction if we identify the 'average' layer thickness e with $c_2/2$. It may seem paradoxical that c_1 cannot be identified with the average layer thickness when interpreting the system as a layer model. The reason becomes clear when the expressions of c_1 and c_2 as a function of D_o, D_p and x are particularized for $D_p = 2D_o$. Under this condition $c_1 = D_o(1+x)$, while $c_2 = 2D_o$. Thus, within the rigid layer model, $e = D_o$, and c_2 is x-independent, the x-dependent misfit between the two subsystems forming the composite being carried out by the x-dependence of c_1. Therefore, the x-dependence of c_2 usually observed in these systems can already be considered a deviation from the layer model, but many other features of this model are maintained and $c_2/2$ can still be identified with the average thickness of the layers.

6 Concluding remarks

The composite modulated model proposed above applies trivially to the commensurate structures at the two limits of the x-range. The case of $A_3A'BO_6$ is depicted in Fig. 19. As $\gamma = 3/4$, its space group $R\bar{3}c$ is in accord with the general results of Table 2. It can be seen in the figure that nearly all atomic positions along the z-axis can be identified trivially with special positions within our general model. Note, for instance, that the positions for the A cations along z correspond to three symmetry-forced zeros of its modulation function. The only free z-component associated with an oxygen is given by the amplitude of the corresponding sawtooth function. One can also see in Fig. 19 that the four possible values (0, 1/4, 1/2 and 3/4) for the initial phase Φ of the modulations (see Table 2) correspond to the four possible different equivalent choices for the initial cell in the sequence of four c_1 unit cells present within the superstructure unit cell. They represent four possible anti-phase domains. A second set of special values for the initial phase (1/8, 3/8, 5/8, 7/8) would describe a different non-equivalent structure, but with the same space group $R\bar{3}c$, as indicated in Table 2.

For the case of the 2H perovskite ABO_3 ($x = 0$), reducing the γ value to 1/2 is not enough. The 2H perovskite has higher symmetry than that expected from Table 2. The reason is that the symmetries of this table are calculated for general modulations fulfilling the superspace symmetry. The necessary additional symmetry of the 2H perovskite is obtained by considering the special layer case of $D_p = 2D_o$ in the oxygen sawtooth functions. This eliminates the z-shift between neighboring columns and is consistent with the fact that hexagonal ABO_3 is a perfect layer structure. As no prism exists

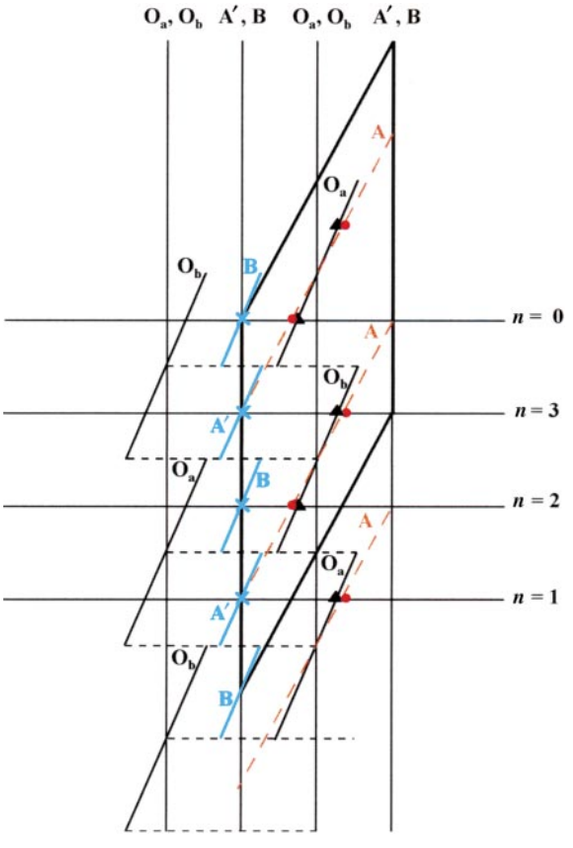

Fig. 19 Graphical superspace representation (projection zx_4) of compounds of the type $A_3A'BO_6$ within the general model of Fig. 13 and 17(a). The discrete points within the modulation functions corresponding to the atomic positions realized in the real space structure are indicated with symbols: red points (A atoms), blue crosses (A′, B atoms) and black triangles (O atoms).

in this structure, D_p becomes undefined except for the condition that it should be adequate to equalize the z-level of oxygens in neighboring columns. Thus, the case $x=0$, although within the general framework, is somehow an isolated case, as for any other composition $x \neq 0$, no matter how close to zero, the existence of a certain number of O_6 prisms along the columns forces us to consider a value for D_p in general quite far from the ideal layer value of $2D_o$.

Summarizing, a general modulated composite model has been proposed as a natural reference for the description of the structures of the compounds $A_{3n+3m}A'_nB_{3m+n}O_{9m+6n}$. A single parameter, besides the composition, defines the modulation functions for all the atoms. These functions are in general of the sawtooth type, similar to those present in one dimensional models of quasicrystals. The proposed structural model generalizes the layer picture and includes local fluctuations of the layer plane due to the mismatch between the sizes of the octahedral and prismatic oxygen polyhedra formed in the structures. The model not only agrees with the main features observed in these structures, but also predicts the sequence of octahedra and prisms along the trigonal $[A',B]O_3$ columns for any composition. These sequences are a generalization of the sequence known as the Fibonacci chain and this is realized for a specific composition. The interaction between the two subsystems of the composite is very strong, with the modulation of the A cations strongly correlated with the modulations of the $[A',B]O_3$ columns that cause the presence of the O_6 prisms. In the cases where the B cations in the compound can have two and four valence states, the phason-type excitations of these systems should have very peculiar features as they would involve atomic flips similar to those observed in quasicrystals correlated with valence switches of some B cations.

References

1 J. Darriet and M. A. Subramanian, *J. Mater. Chem.*, 1995, **5**, 543.
2 J. A. Campá, E. Gutierrez-Puebla, M. A. Monge, I. Rasines and C. Ruiz-Valero, *J. Solid State Chem.*, 1994, **108**, 230.
3 W. T. A. Harrison, S. L. Hegwood and A. J. Jacobson, *J. Chem. Soc., Chem. Commun.*, 1995, 1953.
4 P. D. Battle, G. R. Blake, J. Darriet, J. G. Gore and F. Weill, *J. Mater. Chem.*, 1997, **7**, 1559.
5 J. B. Claridge and H. C. Zur Loye, to be published.
6 P. D. Battle, J. C. Burley, E. J. Cussen, J. Darriet and F. Weill, *J. Mater. Chem.*, 1999, **9**, 479.
7 J. Campá, E. Gutierrez-Puebla, A. Monge, I. Rasines and C. Ruiz-Valero, *J. Solid State Chem.*, 1996, **126**, 27.
8 M. Evain, F. Boucher, O. Gourdon, V. Petricek, M. Dusek and P. Bezdicka, *Chem. Mater.*, 1998, **10**, 3068.
9 C. Dussarrat, J. Fompeyrine and J. Darriet, *Eur. J. Solid State Chem.*, 1995, **32**, 3.
10 P. D. Battle, G. R. Blake, J. Sloan and J. F. Vente, *J. Solid State Chem.*, 1998, **136**, 103.
11 F. Abraham, S. Minaud and C. Renard, *J. Mater. Chem.*, 1994, **4**, 1763.
12 M. Huvé, C. Renard, F. Abraham, G. Van Tendeloo and S. Amelinckx, *J. Solid State Chem.*, 1998, **135**, 1.
13 F. Grasset, F. Weill and J. Darriet, *J. Solid State Chem.*, 1998, **140**, 194.
14 K. Ukei, A. Yamamoto, Y. Watanabe, T. Shishido and T. Fukuda, *Acta Crystallogr., Sect. B.*, 1993, **49**, 67.
15 T. Shishido, K. Ukei and T. Fukuda, *J. Alloys Compd.*, 1996, **237**, 89.
16 J. J. Randall and L. Katz, *Acta Crystallogr.*, 1959, **12**, 519.
17 J. Darriet, F. Grasset and P. D. Battle, *Mater. Res. Bull.*, 1997, **32**, 139.
18 A. P. Wilkinson and A. K. Cheetham, *Acta Crystallogr., Sect. C*, 1989, **45**, 1672.
19 P. Núñez, S. Trail and H. C. Zur Loye, *J. Solid State Chem.*, 1997, **130**, 35.
20 J. B. Claridge, R. C. Layland, R. D. Adams and H. C. Zur Loye, *Z. Anorg. Allg. Chem.*, 1997, **623**, 1131.
21 G. Blake, J. Sloan, J. P. Vente and P. D. Battle, *Chem. Mater.*, 1998, **10,** 3536.
22 M. Evain, *Acta Crystallogr., Sect. B*, to be published.
23 S. Van Smaalen, *Phys. Rev. B*, 1991, **43**, 11330.
24 A. Janner and T. Janssen, *Acta Crystallogr., Sect. A*, 1980, **36**, 399.
25 A. Janner and T. Janssen, *Acta Crystallogr., Sect. A*, 1980, **36**, 408.
26 J. M. Perez-Mato, G. Madariaga, F. J. Zuniga and A. Garcia Arribas, *Acta Crystallogr., Sect. A*, 1987, **43**, 216.
27 S. Van Smaalen, *Crystallogr. Rev.*, 1995, **4**, 79.
28 R. L. Withers, S. Schmid and J. G. Thompson, *Prog. Solid State Chem.*, 1998, **26**, 1.
29 A. Katz and M. Duneau, *J. Phys. (Paris)*, 1986, **47**, 181.
30 P. M. De Wolff, *Acta Crystallogr., Sect. A*, 1974, **30**, 777.
31 A. Janner, T. Janssen and P. M. De Wolff, *Acta Crystallogr., Sect. A*, 1983, **39**, 658.
32 A. Yamamoto, T. Janssen, A. Janner and P. M. De Wolff, *Acta Crystallogr., Sect. A*, 1985, **41**, 528.
33 A. Janner and T. Janssen, *Phys. Rev. B*, 1977, **15**, 643.
34 The Farey series of order 1025, *Royal Society Mathematical Tables, volume I*, University Press, Cambridge, 1950.
35 T. Janssen, *Methods of Structural Analysis of Modulated Structures and Quasicrystals*, ed. J. M. Perez-Mato, F. J. Zuniga and G. Madariaga, World Scientific Singapore, 1991, p. 47.
36 S. Lyonnard, G. Coddens, Y. Calvairac and D. Gratias, *Phys. Rev. B*, 1996, **53**, 3150.

Paper 9/03723C